

Cone Degeneration Following Rod Ablation in a Reversible Model of Retinal Degeneration

Rene Y. Choi,^{1,2} Gustav A. Engbretson,^{1,3} Eduardo C. Solessio,¹ Georgette A. Jones,¹ Adam Coughlin,¹ Ilija Aleksic,¹ and Michael E. Zuber^{1,2}

PURPOSE. Amphibian retinas regenerate after injury, making them ideal for studying the mechanisms of retinal regeneration, but this leaves their value as models of retinal degeneration in question. The authors asked whether the initial cellular changes after rod loss in the regenerative model *Xenopus laevis* mimic those observed in nonregenerative models. They also asked whether rod loss was reversible.

METHODS. The authors generated transgenic *X. laevis* expressing the *Escherichia coli* enzyme nitroreductase (NTR) under the control of the rod-specific rhodopsin (XOP) promoter. NTR converts the antibiotic metronidazole (Mtz) into an interstrand DNA cross-linker. A visually mediated behavioral assay and immunohistochemistry were used to determine the effects of Mtz on the vision and retinas of XOPNTR F₁ tadpoles.

RESULTS. NTR expression was detected only in the rods of XOPNTR tadpoles. Mtz treatment resulted in rapid vision loss and near complete ablation of rod photoreceptors by day 12. Müller glial cell hypertrophy and progressive cone degeneration followed rod cell ablation. When animals were allowed to recover, new rods were born and formed outer segments.

CONCLUSIONS. The initial secondary cellular changes detected in the rodless tadpole retina mimic those observed in other models of retinal degeneration. The rapid and synchronous rod loss in XOPNTR animals suggested this model may prove useful in the study of retinal degeneration. Moreover, the regenerative capacity of the *Xenopus* retina makes these animals a valuable tool for identifying the cellular and molecular mechanisms at work in lower vertebrates with the remarkable capacity of retinal regeneration. (*Invest Ophthalmol Vis Sci.* 2011;52:364–373) DOI:10.1167/iovs.10-5347

Retinitis pigmentosa (RP) is a heterogeneous group of inherited disorders characterized by the initial loss of rod photoreceptors.¹ Rod photoreceptor death is followed by sec-

ondary degenerative changes, the most notable and debilitating of which is the subsequent death of cone photoreceptors.² Other cellular changes include Müller glial cell hypertrophy, synaptic layer loss, and retinal interneuron death.²

Mammalian animal models that mimic aspects of RP have been critical for investigating the mechanisms of rod cell death and the secondary changes that follow.^{3,4} In contrast, amphibian, fish, and, more recently, chicken model systems have been predominantly used to study retinal regeneration because of the remarkable ability of these species to partially or even fully recover from retinal damage.^{5–7} The retinal damage/regeneration paradigms used in lower vertebrates have ranged from complete and partial retinectomy to the ablation of individual retinal cell classes using chemical and genetic approaches.^{5,6,8–14} Given their ability to replace dead or dying retinal cells, we asked whether a regenerative animal model (*Xenopus laevis*) would also exhibit the secondary cellular changes observed in nonregenerative animal models.

To address this question, we generated a transgenic line of *X. laevis* driving the expression of *Escherichia coli* nitroreductase (NTR) under the control of the rod-specific rhodopsin promoter (XOP).^{15,16} Nitroreductase converts nitroimidazole prodrugs, such as metronidazole (Mtz), into a cytotoxic DNA cross-linker.^{17,18} Taking advantage of a low-light, visually based behavioral assay, we show Mtz-treated XOPNTR transgenic tadpoles rapidly lose their vision.^{19,20} Rod cell death is swift, specific, and parallels the loss in sight. Apoptotic rods were detected at 24 hours, and rod outer segment degeneration was extensive by 5 days. Müller cell hypertrophy and cone photoreceptor degeneration and death followed rod degeneration. Furthermore, new rod photoreceptors were generated after selective rod ablation. These results suggest that retinal degeneration after rod loss in Mtz-treated XOPNTR animals mimics retinal degeneration in other animal models, despite the ability of *Xenopus* to regenerate all retinal cell classes. Consequently, *Xenopus* may serve not only as a model system for retinal development and regeneration but also for understanding the cellular and molecular mechanisms of retinal degeneration.

METHODS

Generation of XOPNTR Transgene and Transgenic Animals

The transgene construct pXOP(–508/+41)-NTR was generated by replacing eGFP of pXOP(–508/+41)GFP with the *E. coli* NTR gene from plasmid F116.¹⁶ XOPNTR F₀ transgenic *X. laevis* were generated using restriction enzyme-mediated integration, and four XOPNTR founders, two males and two females, were grown to adulthood.²¹ Progeny from the founder females, XOPNTR1 and XOPNTR2, were generated, and only XOPNTR2 tadpoles responded to metronidazole treatment.

From the Departments of ¹Ophthalmology and ²Biochemistry and Molecular Biology, Center for Vision Research, SUNY Eye Institute, Upstate Medical University, Syracuse, New York; and the ³Department of Biomedical and Chemical Engineering, Syracuse University, Syracuse, New York.

Supported by National Institutes of Health Grants EY015748 and EY017964 (MEZ); Research to Prevent Blindness Career Development Award (MEZ) and unrestricted grant to the Upstate Medical University Department of Ophthalmology; the E. Matilda Zeigler Foundation for the Blind (MEZ); and the Lions of Central New York.

Submitted for publication February 8, 2010; revised June 26 and July 17, 2010; accepted August 2, 2010.

Disclosure: **R.Y. Choi**, None; **G.A. Engbretson**, None; **E.C. Solessio**, None; **G.A. Jones**, None; **A. Coughlin**, None; **I. Aleksic**, None; **M.E. Zuber**, None

Corresponding author: Michael E. Zuber, Departments of Ophthalmology and Biochemistry and Molecular Biology, SUNY Upstate Medical University, 750 East Adams Street, Syracuse, NY 13210; zuberem@upstate.edu.

Generation of F₁ Tadpoles and Genotyping

The transgenic female was injected 1 week and 1 day before egg collection with pregnant mare's serum gonadotropin (Sigma Aldrich, St. Louis, MO) and human chorionic gonadotropin (Intervet, Millsboro, DE), respectively, to induce egg laying, and the eggs were fertilized in vitro using wild-type sperm. DNA from tail snips of F₁ tadpoles was isolated (DNeasy Blood and Tissue Kit; Qiagen Inc., Valencia, CA). Primers specific for the XOPNTR transgene (5' XOPNTR, 5'-CGCTA-AATCCTTTGTTGCTGACGC-3'; 3' XOPNTR, 5'-GTTGAACACGTAAT-TACCGGCAGC-3') were used to identify transgenic tadpoles and their nontransgenic siblings, which were used as wild-type controls. The Committee for the Humane Use of Animals at SUNY Upstate Medical University approved all procedures, and all procedures adhered to the ARVO Statement for the Use of Animals in Ophthalmic and Vision Research.

Metronidazole Preparation and Use

Metronidazole (Sigma Aldrich; product no. M-1547) was dissolved in 0.1× MMR containing 0.4% dimethyl sulfoxide (DMSO; Sigma-Aldrich; product no. D8418) to a final concentration of 10 mM immediately before use.²² Control animals were cultured in the same solution without Mtz. Preliminary experiments demonstrated that higher concentrations of Mtz were toxic. No more than 30 stage 50 to stage 53 (stages are noted in figure legends) transgenic or nontransgenic sibling tadpoles were cultured in 600 mL Mtz solution and raised at 22°C in complete darkness (Mtz is light sensitive) for the indicated time. Preliminary experiments demonstrated that there were no differences in the response to Mtz for tadpoles between stages 50 and 53. For regeneration experiments, animals were Mtz-treated then allowed to recover for periods of up to 30 days in 0.1× MMR in ambient laboratory lighting.

Cryosectioning, Immunohistochemistry, and In Situ Hybridizations

Tadpoles were euthanized in 1% methanesulfonate (Tricaine; Sigma-Aldrich), fixed in 4% paraformaldehyde for 1 hour, immersed in 20% sucrose, mounted in OCT, and cryostat sectioned (12 μm). When staining for rod transducin, animals were incubated for 2 hours in room light to ensure labeling of rod somata. The following primary antibodies were used for immunostaining: anti-transducin polyclonal (1:100; product no. sc-389; Santa Cruz Biotechnology, Santa Cruz, CA), anti-XAP2 monoclonal (1:10; clone 5B9; Developmental Studies Hybridoma Bank [DSHB], Iowa City, IA), anti-calbindin polyclonal (1:500; product no. 80001-624; VWR, West Chester, PA), anti-islet-1 monoclonal (1:100; clone 39.4D5; DSHB), anti-calretinin polyclonal (1:100; product no. NB200-618; Novus Biologicals, Littleton, CO), anti-GABA polyclonal (1:500; product no. 20094; Immunostar, Hudson, WI), mouse R5 monoclonal (1:5; kindly provided by W.A. Harris, Cambridge University), and anti-vimentin monoclonal (1:50; clone 14h7; DSHB). The following secondary antibodies tagged with fluorescent molecules were used for immunostaining: goat anti-mouse IgM Alexa 555 (1:500; product no. A-21426), donkey anti-rabbit IgG Alexa 488 (1:500; product no. A-21206), goat anti-mouse IgG Alexa 488 (1:500; product no. A-11001), goat anti-mouse IgG3 Alexa 594 (1:750; product no. A-21155), goat anti-mouse IgG2b Alexa 555 (1:500; product no. A-21147), and goat anti-mouse IgG1 Alexa 488 (1:500; product no. A-21121). All secondary antibodies were purchased from Invitrogen (Carlsbad, CA). In situ hybridizations were performed as previously described.²³ Substrate (Fast Red; Roche Applied Science, Indianapolis, IN) was used for the in situ hybridization procedure. The slides were mounted in a solution of reagent (FluorSave; VWR), 2% 1,4-diazabicyclo[2.2.2]octane (DABCO; Sigma-Aldrich), and 10 mg/mL 4,6-diamidino-2-phenylindole, dilactate (DAPI; Sigma-Aldrich).

EdU Labeling

EdU (5-ethynyl-2'-deoxyuridine; 10 mM) was injected intra-abdominally on days 3 and 10 of Mtz treatment and on days 3, 10, and 21

during recovery. On day 30 of recovery, animals were processed for immunohistochemistry, as described, and then for EdU using an Alexa-Fluor 488 imaging kit according to the manufacturer's instructions (Click-iT EdU; product no. C10337; Invitrogen).

TUNEL Cell Apoptosis Assay

Dying cells were detected with an in situ apoptosis detection kit in accordance with the manufacturer's instructions (ApopTag Red; product no. S7165; Millipore, Billerica, MA). A rhodamine-conjugated primary antibody was used to detect labeled cells.

Imaging and Cell Counts

Stained sections were visualized using an upright fluorescence light microscope with motorized Z-focusing (DM6000 B; Leica Microsystems, Bannockburn, IL) fitted with a camera (Retiga-SRV; Q-Imaging, Surrey, BC, Canada) for image capture. Images were processed (Velocity software, version 5.0.3; Improvion Inc., a PerkinElmer Company, Waltham, MA). For each treatment group, no fewer than three animals were used. A single central retinal section from each animal was scored. In Figure 6, a region between the ventro-temporal and the central retina was selected for scoring. Cells were counted within a region spanning 100 μm. Unless otherwise noted, *n* equals the number of animals analyzed (**P* ≤ 0.05; ***P* ≤ 0.01). Statistical analysis was performed using a Student's *t*-test, paired two-tailed distribution.

Dim-Light Visually Mediated Behavioral Assay

Behavioral assays were performed as previously described with several changes.¹⁹ Stage 50 tadpoles were housed individually during drug treatment and behavioral testing. Twelve hours before testing, tanks containing transgenic or control animals were wrapped in aluminum foil (Mtz-treated tadpoles and their respective controls were exposed to room light during feeding and, therefore, had to be dark adapted). The behavioral response was recorded with a digital camcorder using infrared illumination for off-line analysis. (Preliminary experiments demonstrated the infrared light source on the camcorder did not elicit a behavioral response.) Stimulus light was provided from a 70-W tungsten-halide lamp collimated and attenuated in 0.5-log increments with neutral density filters. The beam was focused onto the entrance aperture of a fiberoptics light pipe. The light pipe terminated in a ring illuminator (2-inch inside diameter, 3.5-inch outside diameter; product no. NT54-173; Edmund Optics, Barrington, NJ) centered 9 inches above the tank housing the tadpoles. Maximal luminance at the tank was 120 photometric cd/m² measured with a photometer (model 370; Graseby Optronics, Orlando, FL). See Supplementary Movie S1, <http://www.iovs.org/lookup/suppl/doi:10.1167/iovs.10-5347/-DCSupplemental>, for further details and an example of the response observed before and after Mtz treatment. Calculations used to determine the light threshold needed to elicit the observed response can be found in the Supplementary Text, <http://www.iovs.org/lookup/suppl/doi:10.1167/iovs.10-5347/-DCSupplemental>. Results in figures are shown as the mean percentage of time spent on the white side of the tank ± SE mean. A two-tailed Student's *t*-test with *P* ≤ 0.05 was considered significant.

RESULTS

Expression of Nitroreductase in Rod Photoreceptors of F₁ XOPNTR Tadpoles

We generated F₀ transgenic *X. laevis* expressing NTR under the control of the -508 to +41 region of the *X. laevis* rhodopsin promoter (XOP).^{16,24} Transgenics were identified by genotyping using XOPNTR-specific PCR primers, then grown to adulthood. Tadpoles generated from one founder female (XOPNTR) were used for all experiments in this study.

In situ hybridization was used to determine the expression pattern of NTR in stage 50 F₁ tadpoles. Consistent with the known activity of the -508 to +41 region of the rhodopsin

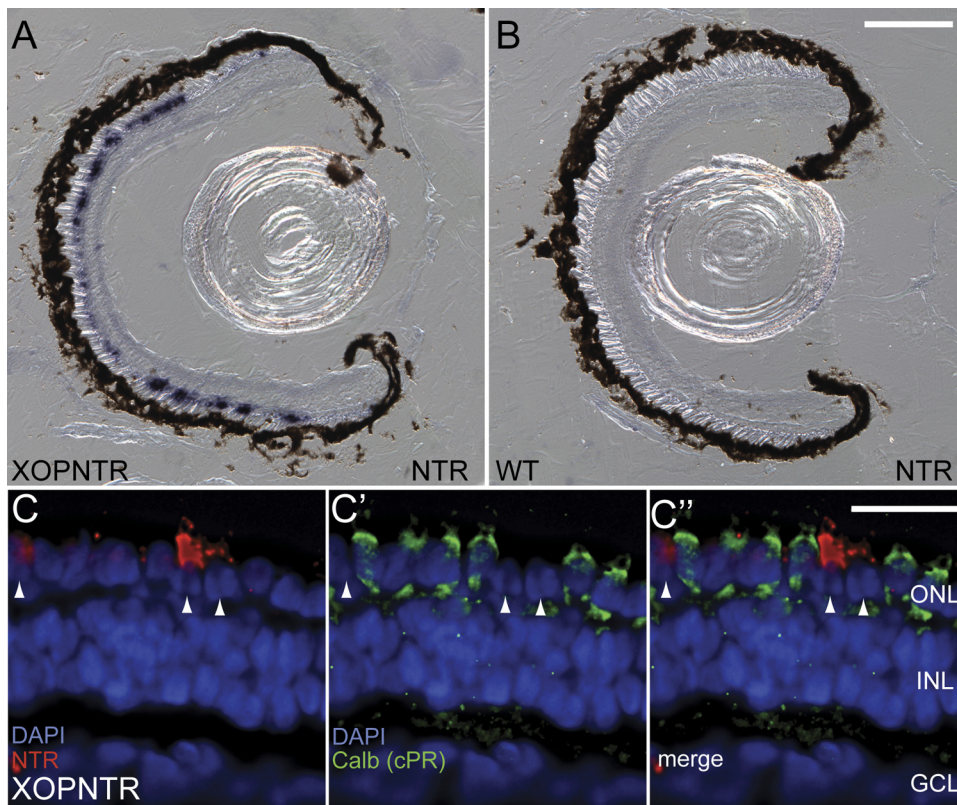


FIGURE 1. NTR expression in rod photoreceptors of stage 50 F_1 XOPNTR tadpoles. (A, B) In situ hybridization was used to detect NTR expression (purple) in transgenic and control tadpoles. NTR expression was detected in the outer nuclear layer of XOPNTR tadpoles (A) but was undetectable in wild-type sibling embryos (B). (C–C'') Retinas were triple stained to label NTR-expressing cells (Fast red; red), cones (calbindin; green), and nuclei (DAPI; blue). NTR-expressing cells (C, arrowheads) do not express calbindin (C', C''). Scale bars: 100 μm (A, B); 25 μm (C–C'').

gene, NTR expression was detected only in the outer nuclear layer (ONL) of transgenic tadpoles (Fig. 1A; $n = 4$).²⁴ In contrast, NTR was undetectable in wild-type (nontransgenic sibling) retinas (Fig. 1B; $n = 4$). The intensity and distribution of NTR expression in the ONL varied from animal to animal, consistent with previous reports attributing these differences to position-effect variegation, which can result in altered transgene expression on the order of days or even hours in genetically nonmosaic animals.²⁵ To determine whether NTR expression was detectable in cone photoreceptors, retinas were costained for the NTR transcript and calbindin, which specifically labels cone photoreceptors in *Xenopus*.²⁶ NTR expression was never detected in cones (156 cells from four retinas; Figs. 1C, 1C', and 1C''), suggesting that NTR expression was rod photoreceptor specific.

Rapid Vision Loss and Rod Photoreceptor Ablation in Mtz-Treated XOPNTR Tadpoles

Nitroreductase reduces the antibiotic Mtz to a cytotoxic DNA cross-linker.¹⁷ Therefore, Mtz treatment of transgenic tadpoles should result in rod photoreceptor ablation. We used both a visually based behavioral assay and immunohistochemistry to determine the effect of Mtz on rod cell function and viability in control and XOPNTR transgenic tadpoles (Fig. 2). The behavior and retinal histology of nontransgenic, sibling tadpoles generated from XOPNTR adults and wild-type tadpoles were indistinguishable (not shown). Therefore, nontransgenic tadpoles generated from the same clutch of XOPNTR eggs were used as controls and are labeled here as wild-type.

Transgenic and control tadpoles were cultured in 10 mM Mtz for 17 days. At 6-day intervals, the effect of Mtz treatment on the dim light vision of tadpoles was determined using a modified visually mediated behavioral assay.^{19,20} The behavioral responses of untreated XOPNTR tadpoles and controls were similar (Fig. 2A, day 0). In contrast, we observed a significant drop in the behav-

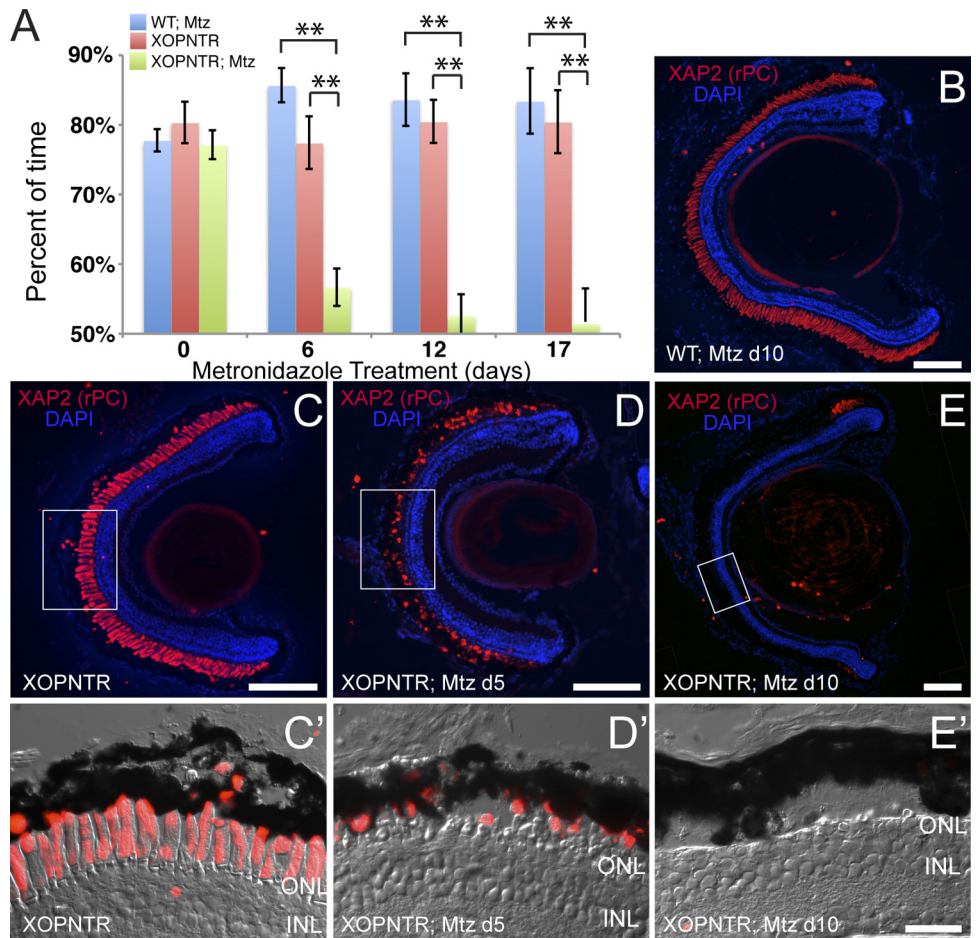
ioral response of Mtz-treated XOPNTR transgenic tadpoles in as little as 6 days (Fig. 2A; $n = 17$). By day 12, Mtz-treated XOPNTR animals were unable to distinguish between the white and black sides of the test tank ($n = 14$). In contrast, the responses of DMSO-only treated XOPNTR transgenic ($n = 5$) and Mtz-treated wild-type tadpoles ($n = 6$) were unchanged.

Immunohistochemistry using the rod-specific XAP2 antibody was used to determine the effect of Mtz on rod cells.²⁷ The morphology of rods in Mtz-treated wild-type ($n = 14$) and untreated XOPNTR tadpoles ($n = 16$) was normal (Figs. 2B, 2C, 2C'). In contrast, the retinas of all Mtz-treated, XOPNTR tadpoles were severely altered. At 5 days, rod outer segments were reduced in number, shorter, and fragmented (Figs. 2D, 2D'; $n = 8$). After 10 days of exposure there was a near complete lack of rod outer segments (Figs. 2E, 2E'; $n = 15$). Intact rod outer segments were sometimes, but not consistently, observed in the most peripheral region of the retina (Fig. 2E; $n = 15$). However, no consistent pattern of rod loss was observed. Together, these results suggest Mtz treatment results in vision loss because of rapid rod outer segment degeneration and possibly rod photoreceptor ablation in XOPNTR animals.

Apoptotic Cell Death Is Initially Photoreceptor Specific in Mtz-Treated XOPNTR Tadpoles

The restricted expression pattern of NTR predicts rod photoreceptors would be primarily affected by Mtz treatment. To determine which retinal cell classes were initially affected, stage 53 tadpoles were cultured in Mtz for 1 day and apoptotic cells were identified using terminal deoxynucleotidyl transferase-mediated deoxyuridine triphosphate nick end-labeling (TUNEL) detection. TUNEL-positive cells were seldom observed in either Mtz-treated wild-type or untreated XOPNTR tadpoles (Figs. 3A, 3B). In the retinas of untreated XOPNTR tadpoles, TUNEL-positive cells were infrequently observed in the ganglion cell layer (GCL; 0.5% of cells; $n = 7$), whereas the

FIGURE 2. Rapid vision loss and rod outer segment loss in Mtz-treated stage 50 XOPNTR tadpoles. (A) A behavioral assay was used to determine the effect of metronidazole on the dim-light vision of XOPNTR transgenic tadpoles and their wild-type (WT) siblings. Histogram bars indicate the average percentage of time spent on the white side of the test tank. Blue, red, and green bars denote wild-type Mtz-treated, XOPNTR DMSO-treated (referred to as untreated), and XOPNTR Mtz-treated tadpoles, respectively. The mean \pm SEM is indicated. The behavioral responses of WT Mtz-treated and XOPNTR untreated animals were not statistically different at any time point, whereas the Mtz-treated animals were significantly different from both control groups on treatment days 6, 12, and 17. Immunohistochemistry was used to determine the effect of Mtz treatment on rod photoreceptors. Retinal sections were stained to detect rod photoreceptor outer segments (XAP2; red) and cell nuclei (DAPI; blue). Wild-type (B) and transgenic (C–E) tadpoles were treated for 5 days with DMSO only (C) or for 5 or 10 days with Mtz (B, D, E). Higher magnification views of the boxed regions in C–E are shown in C'–E'. Scale bars: 100 μ m (B–E); 25 μ m (C'–E'). $**P \leq 0.01$.



only TUNEL-positive cells detected in Mtz-treated wild-type animals were located in the inner nuclear layer (INL; 0.4% of cells; $n = 10$). Although a similarly small number of INL cells were apoptotic in the retinas of Mtz-treated XOPNTR animals (0.4% of INL cells), we observed dramatic cell death in the outer nuclear layer (Fig. 3C; $n = 8$).

To determine the extent to which rods and cones were affected, we costained retinas for TUNEL and cone calbindin.

No TUNEL-positive cells were detected in the central retina ONL of either Mtz-treated wild-type or untreated XOPNTR tadpoles. In contrast, in Mtz-treated XOPNTR tadpoles, 50.3% of rods but only 3.4% of cone nuclei were TUNEL-positive (Figs. 3D, 3D', 3D'').

The *Xenopus* retina contains approximately equivalent numbers of rod and cone photoreceptors. Therefore, these results suggest nearly 15-fold more rods than cones are TUNEL-

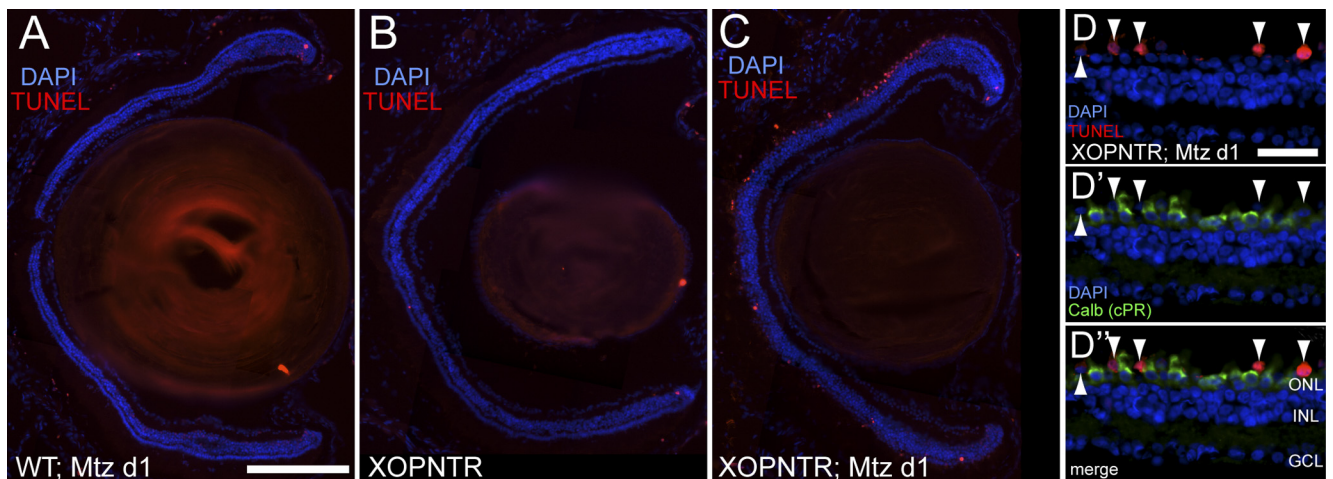


FIGURE 3. Rapid rod cell death in stage 53 transgenic XOPNTR tadpoles treated with metronidazole. (A–C) Retinal sections were labeled to detect apoptotic cells (TUNEL; red) and all cell nuclei (DAPI; blue). Wild-type (A) and transgenic (B, C) tadpoles were left untreated (B) or were treated with Mtz (A, C) for 1 day. (D–D'') To identify the class of apoptotic cells in the ONL, retinal sections were stained for TUNEL (D; red) and the cone marker calbindin (D'; green). D and D' are merged in D''. Scale bars: 200 μ m (A–C); 25 μ m (D–D''). Arrowheads: TUNEL-positive cells.

positive after 1 day of treatment. This is to be expected because NTR should only be expressed in rods given that it is under the control of the rhodopsin promoter. Another explanation for the relatively low number of TUNEL-positive cones is that cones might have been rapidly killed, cleared from the retina, and therefore not detected. To test this hypothesis, we compared the number of cones in treated and control transgenic animals. We found no statistically significant difference in the number of cones after 1 day of Mtz-treatment (XOPNTR untreated 20.1 ± 0.8 , XOPNTR Mtz-treated 20.5 ± 1.2 ; $P > 0.79$). Taken together, these results suggest rod photoreceptors are the initial and predominant cell type ablated in Mtz-treated XOPNTR tadpoles.

Progressive Cone Outer Segment Degeneration and Death Follow Rod Ablation

In mammals, cone degeneration follows rod cell loss. We wondered whether a similar dynamic was detectable in the

Xenopus retina. XOPNTR tadpoles were treated with Mtz for 1, 3, 5, 10, and 17 days. The total number and the percentage of TUNEL-positive rods and cones were determined at each time point. Rod transducin and cone calbindin were used to label photoreceptors because these markers are detected in both the outer segments and the somata of these respective cell types. No change in the number of rods or cones was observed in XOPNTR tadpoles during the first 3 days of Mtz treatment (rods: day 0, 21.6 ± 1.2 [$n = 7$] vs. day 3, 21.0 ± 0.6 [$n = 3$]; cones: day 0, 15.4 ± 0.9 [$n = 7$] vs. day 3, 15.0 ± 1.5 [$n = 3$]). Similar rod (20.6 ± 0.9 ; $n = 7$) and cone (15.9 ± 0.6 ; $n = 7$) numbers were detected in age-matched nontransgenic siblings. However, 93.7% of rods and only 6.7% of cones were TUNEL-positive on day 3. By day 5, rod cell loss was obvious, and by day 10, the few remaining rods (0.7 ± 0.7 ; $n = 3$) were all TUNEL-positive (Fig. 4A). Rod transducin was undetectable on day 17 of treatment. By comparison, the number of cones was unchanged through day 10 of

A

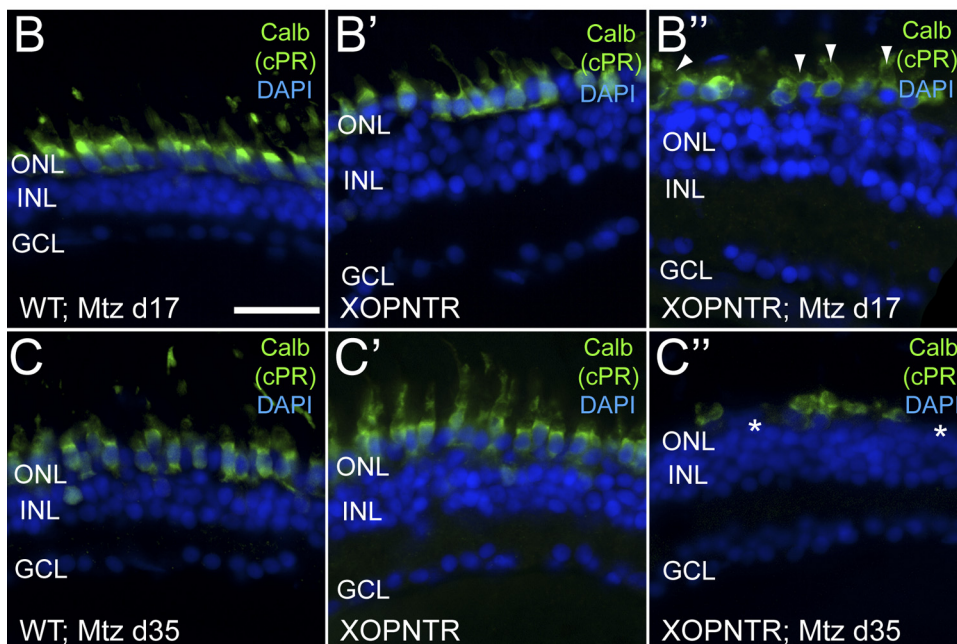
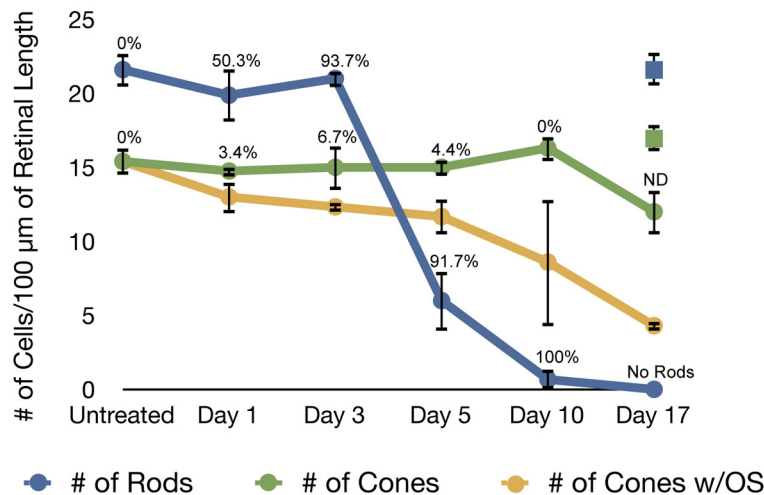


FIGURE 4. Cones degenerate after rod ablation. Stage 52 XOPNTR tadpoles were treated with Mtz for 1 to 17 days. Retinal sections were stained for rods (transducin), cones (calbindin), apoptotic cells (TUNEL), and nuclei (DAPI). The blue, green, and orange lines indicate the number of rods, cones, and cones with outer segments over time, respectively. The percentage of TUNEL-labeled cells at each time point is shown. The numbers of rods (blue) and cones (green) in control wild-type animals treated with Mtz for 17 days are shown for comparison (all cones had outer segments). Similar results were observed in transgenic control animals treated with DMSO for 17 days (18.3 ± 0.9 rods; 16.3 ± 0.9 cones). Retinal sections of wild-type Mtz-treated (B, C), XOPNTR untreated (B', C') and XOPNTR Mtz-treated (B'', C'') tadpoles were stained for calbindin. Animals were treated for either 17 (B, B'') or 35 (C, C'') days. All sections were counterstained for nuclei (DAPI). Asterisks: region lacking an outer plexiform layer (C''). Arrowheads: cones with outer segments. ND, not determined. Scale bar, 20 μm.

treatment (compare day 0 [15.4 ± 0.9] with day 10 [16.3 ± 0.9]), and the percentage of TUNEL-positive cones remained relatively constant (Fig. 4A). No cone cell loss was detected until day 17 of treatment (Fig. 4A).

In mammalian model systems, cone outer segment loss precedes and is an indicator of pending cone cell death.^{2,28,29} Therefore, we also monitored cone outer segment loss in Mtz-treated XOPNTR tadpoles. A progressive reduction in the number of cones with outer segments was observed from day 0 (15.4 ± 0.9 ; $n = 7$) through day 10 (8.7 ± 4.3 ; $n = 3$), despite no apparent change in the total number of calbindin-positive cells (Fig. 4A). By day 17, approximately one-third of surviving cones had outer segments ($n = 8$; Fig. 4A). To determine whether more prolonged exposure to Mtz would result in more dramatic cone outer segment degeneration, we treated XOPNTR transgenics for 17 and 35 days and stained central retinal sections for calbindin. In contrast to retinas from 35-day controls (100% of the cones had outer segments) and 17-day Mtz-treated XOPNTR animals (38% of the cones had outer segments), the retinas of transgenics treated for 35 days lacked cone outer segments (Figs. 4B'' - 4C''; compare with calbindin-positive cells with outer segments: wild-type Mtz-treated, 20.5 ± 1.2 [$n = 4$]; XOPNTR untreated, 19.8 ± 0.6 [$n = 5$]; XOPNTR Mtz-treated, 0 [$n = 4$]). In addition, the retinas of Mtz-treated XOPNTR tadpoles lacked a distinct outer plexiform layer (OPL) compared with control retinas. Small patches of calbindin-positive cone somata were separated by acellular gaps in the ONL in the retinas of Mtz-treated XOPNTR tadpoles (Figs. 4C'', asterisks).

Together, these results suggest the rapid loss of rod photoreceptors followed by more gradual cone outer segment degeneration, and eventually cone cell death, in Mtz-treated XOPNTR tadpoles.

Secondary Cellular Changes in the Rodless Tadpole Retina

In addition to cone loss, other secondary retinal changes follow rod photoreceptor death in all nonregenerative animal models. To determine whether this was also true in the rodless tadpole retina, stage 52 XOPNTR transgenics were cultured in Mtz for 17 days, and immunostaining for neuronal and glial markers was used to identify retinal cell classes. Markers used included islet-1 (retinal ganglion and a subset of inner nuclear layer cells), γ -aminobutyric acid (GABA; horizontal and GABAergic amacrine cells), calretinin (bipolar, GABAergic and serotonergic amacrine and a subset of retinal ganglion cells), R5 and vimentin (Müller glia), and calbindin.³⁰⁻³⁴ The number of cells stained for each marker was determined and compared with results from control untreated XOPNTR and Mtz-treated wild-type animals. Only the number of calbindin-positive cells (cones) differed significantly when the retinas from control and Mtz-treated XOPNTR animals were compared (Fig. 5A and Supplementary Fig. S1, <http://www.iovs.org/lookup/suppl/doi:10.1167/iovs.10-5347/-DCSupplemental>).

The number of Müller glia was unchanged in rodless retinas (Fig. 5A; wild-type Mtz-treated, 8.0 ± 0.2 [$n = 7$]; XOPNTR-untreated, 8.9 ± 0.4 [$n = 7$]; XOPNTR Mtz-treated, 8.5 ± 0.3 [$n = 8$]). However, the morphology of Müller cells was dramatically altered in Mtz-treated transgenic animals. We observed a time-dependent increase in R5 immunoreactivity in the retinas of Mtz-treated XOPNTR transgenic animals (Figs. 5D-G). The increase in R5 staining was most notable in the outer nuclear (Figs. 5D-G, asterisks) and ganglion cell (Figs. 5D-G, double asterisks) layers. An increase in R5 immunoreactivity with no apparent change in Müller cell number could result from either cell hypertrophy or an increase in the expression of the protein recognized by the R5 monoclonal

antibody (the R5 epitope is unknown). To distinguish between these two possibilities, we stained control and day 17 treated retinas with a second Müller cell marker, vimentin.³⁴ We observed no change in the number of vimentin-positive cells in rodless day 17 tadpoles (wild-type Mtz-treated, 9.2 ± 0.4 [$n = 6$]; XOPNTR untreated, 9.1 ± 0.4 [$n = 8$]; XOPNTR Mtz-treated, 9.0 ± 0.2 [$n = 7$]). As with R5, vimentin staining was unchanged in controls but was dramatically increased in degenerating retinas (not shown), suggesting hypertrophy of Müller cells is also a secondary effect of rod cell loss in Mtz-treated XOPNTR transgenic tadpoles.

Regeneration of Rod Photoreceptors after Mtz Removal

The retinas of *X. laevis* frogs can completely regenerate after partial or complete retinectomy.^{6,11,14} To determine whether rod loss was reversible in the intact retinas of transgenic XOPNTR tadpoles, stage 53 tadpoles were treated with Mtz for 12 days and allowed to recover for 30 days.

XOPNTR transgenic animals treated with Mtz showed no central retina XAP2 staining (Figs. 6A, A'; $n = 4$). The only rod outer segments detected were located in the most peripheral region of the outer nuclear layer immediately adjacent to the ciliary marginal zone (CMZ) and consisted, on average, of fewer than five cells per section (Fig. 6A; asterisk). As expected, rod outer segments of both control groups were unaffected (not shown; $n = 4$ for both wild-type treated and XOPNTR untreated groups). After 30 days of recovery, XAP2-positive rod outer segments were once again observed in Mtz-treated XOPNTR transgenic animals (compare Figs. 6A, A' with 6B, B'). Rods were detected throughout the outer nuclear layer, but their regeneration was incomplete, with some rodless regions persisting (Fig. 6B, arrowheads; $n = 3$). Compared with the long finger-like outer segments of control retinas (Figs. 6C', 6D'), the regenerated rod outer segments were shorter and wider in appearance, resembling the immature rods of younger retinas (Fig. 6B'). We compared the number of ONL nuclei in Mtz-treated XOPNTR tadpoles with those of controls. Metronidazole treatment reduced the number of ONL nuclei by approximately 50% (XOPNTR untreated 12 days, 38.7 ± 1.7 [$n = 3$]; XOPNTR Mtz-treated 12 days, 19.5 ± 1.6 [$n = 3$]). After recovery, the density of nuclei in ONL regions containing rod outer segments was similar to that of untreated transgenics, suggesting the new outer segments are generated from newly born rod photoreceptors (XOPNTR untreated 12 days, recovery 30 days, 39.7 ± 0.7 [$n = 3$]; XOPNTR Mtz-treated 12 days, recovery 30 days, 40.7 ± 0.3 [$n = 3$]).

The marker XAP2 labels only rod outer segments. Therefore, regenerated outer segments could originate from either newly born rods or from undetected rod somata that had lost their outer segments. To distinguish between these possibilities, we treated XOPNTR tadpoles with Mtz for 17 days, allowed them to recover for 30 days, and periodically injected the animals with the thymidine analog EdU, which is incorporated into the DNA of replicating cells during S phase. Transducin-expressing cells were not detected in the central retinas of Mtz-treated XOPNTR tadpoles (Fig. 6E). Similar to the XAP2 staining, transducin was only detected in the most peripheral retina, immediately adjacent to the CMZ (two to three cells on average per section, not shown). By comparison, transducin was strongly expressed in both the soma and the outer segments of control rods (compare Figs. 6E and 6G: XOPNTR Mtz-treated, 0 ± 0 [$n = 3$] vs. XOPNTR untreated, 19.3 ± 0.3 [$n = 3$]). Transducin-positive rods were once again observed in Mtz-treated transgenics after a 30-day recovery phase (compare Figs. 6E and 6F; XOPNTR Mtz-treated 17 days, recovery 30 days, 5.2 ± 1.3 [$n = 5$]). Importantly, 65.4% of the rods

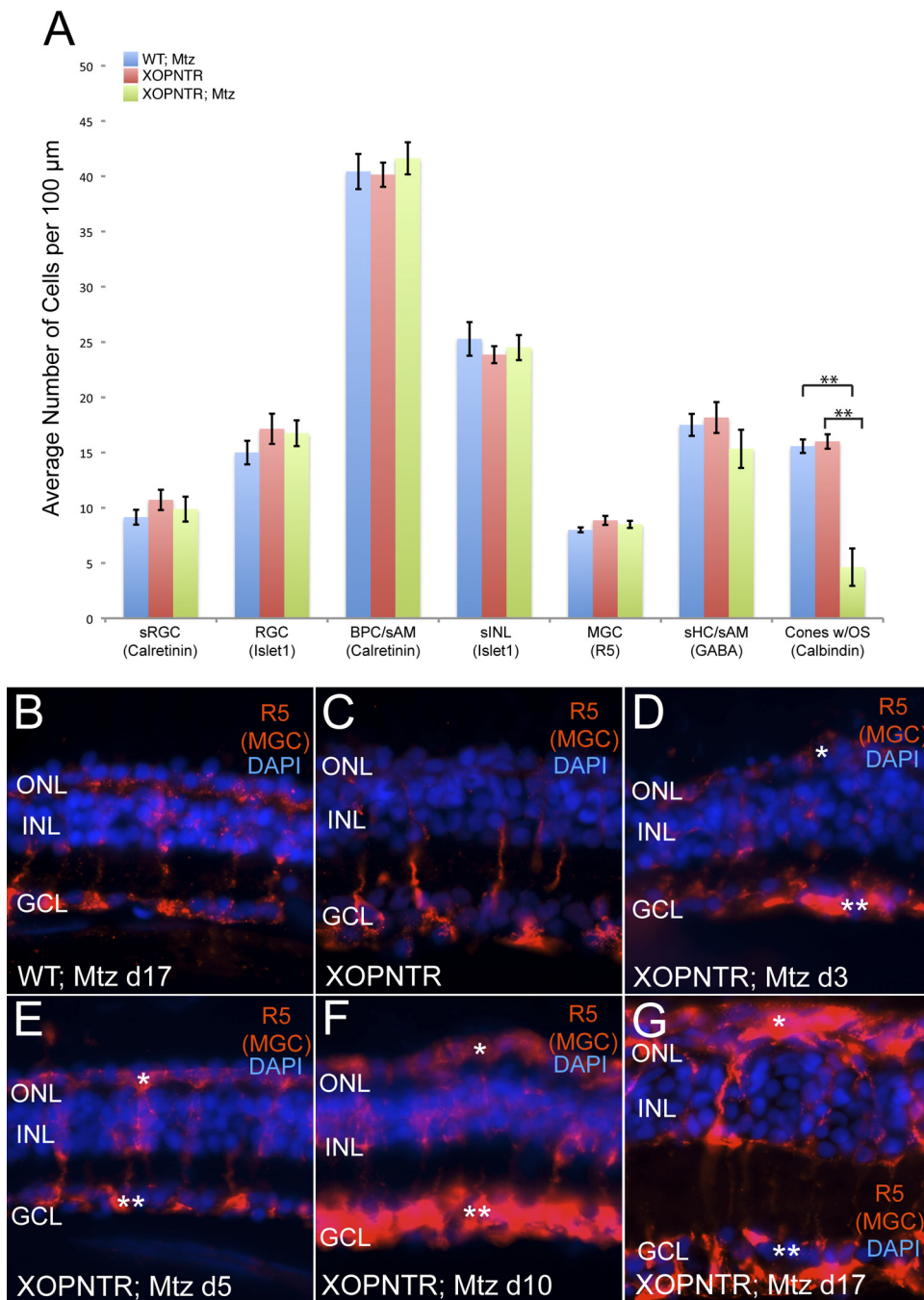


FIGURE 5. Secondary changes follow rod photoreceptor ablation. The retinas of control and XOPNTR stage 52 tadpoles treated with Mtz for 17 days were immunostained with retinal cell markers. (A) Blue, red, and green bars indicate the average number of cells detected in wild-type Mtz-treated, XOPNTR untreated, and XOPNTR Mtz-treated tadpoles for each respective marker. (B–G) Retinal sections of wild-type Mtz-treated (B), XOPNTR untreated (C), and XOPNTR Mtz-treated (D–G) tadpoles stained for R5 (Müller glia). Animals were treated for 3 (D), 5 (E), 10 (F), and 17 (G) days. All sections were counterstained for nuclei (DAPI). *Single asterisks*: Müller cell gliosis spreading to the subretinal layer. *Double asterisks*: Müller cell gliosis spreading to the GCL. RGC, retinal ganglion cells; sRGC, subset of retinal ganglion cells; BPC, bipolar cells; sAM, subset of amacrine cells; sHC, subset of horizontal cells; sINL, subset of inner nuclear layer cells; MGC, Müller glial cells. $^{***}P < 0.0001$. Scale bar, 20 μm . See also Supplementary Fig. S1, <http://www.iovs.org/lookup/suppl/doi:10.1167/iovs.10-5347/-/DCSupplemental>.

observed were EdU-positive, demonstrating these outer segments were generated by newly born rods (Fig. 6F; XOPNTR Mtz-treated 17 days, recovery 30 days, 65.4% EdU+ [$n = 5$] vs. control XOPNTR untreated 17 days, recovery 30 days, 1.5% EdU+ [$n = 4$]). Together, these results indicate that rod loss is reversible in XOPNTR transgenic tadpoles. Within 30 days of rod ablation, new rods were born and generated outer segments.

DISCUSSION

We report that in spite of its regenerative capacity, rod photoreceptor loss in *X. laevis* results in secondary cellular changes similar to those observed in nonregenerative models. Cone cell degeneration and death are observed in patients with

RP and in all nonregenerative RP animal models.^{2,35–43} Similarly, ablation of rod photoreceptors using the NTR-metronidazole enzyme-prodrug system resulted in outer segment degeneration and cone cell death in *X. laevis* (Fig. 4). In contrast to these results, a recent study also using *X. laevis* did not report cone loss after rod cell ablation.⁹ Activation of a modified caspase-9 (iCasp9) in rod photoreceptors resulted in rod cell death in both premetamorphic and postmetamorphic *X. laevis*. Although cone death was not reported, cone function was compromised after 3 months in postmetamorphic animals. Interestingly, photopic ERGs recovered by 5 months, prompting the speculation that recovery resulted from either functional restoration or regeneration of cones. The differences observed in these two *Xenopus* models might have been due to the enzyme-prodrug system used, the time at which it was

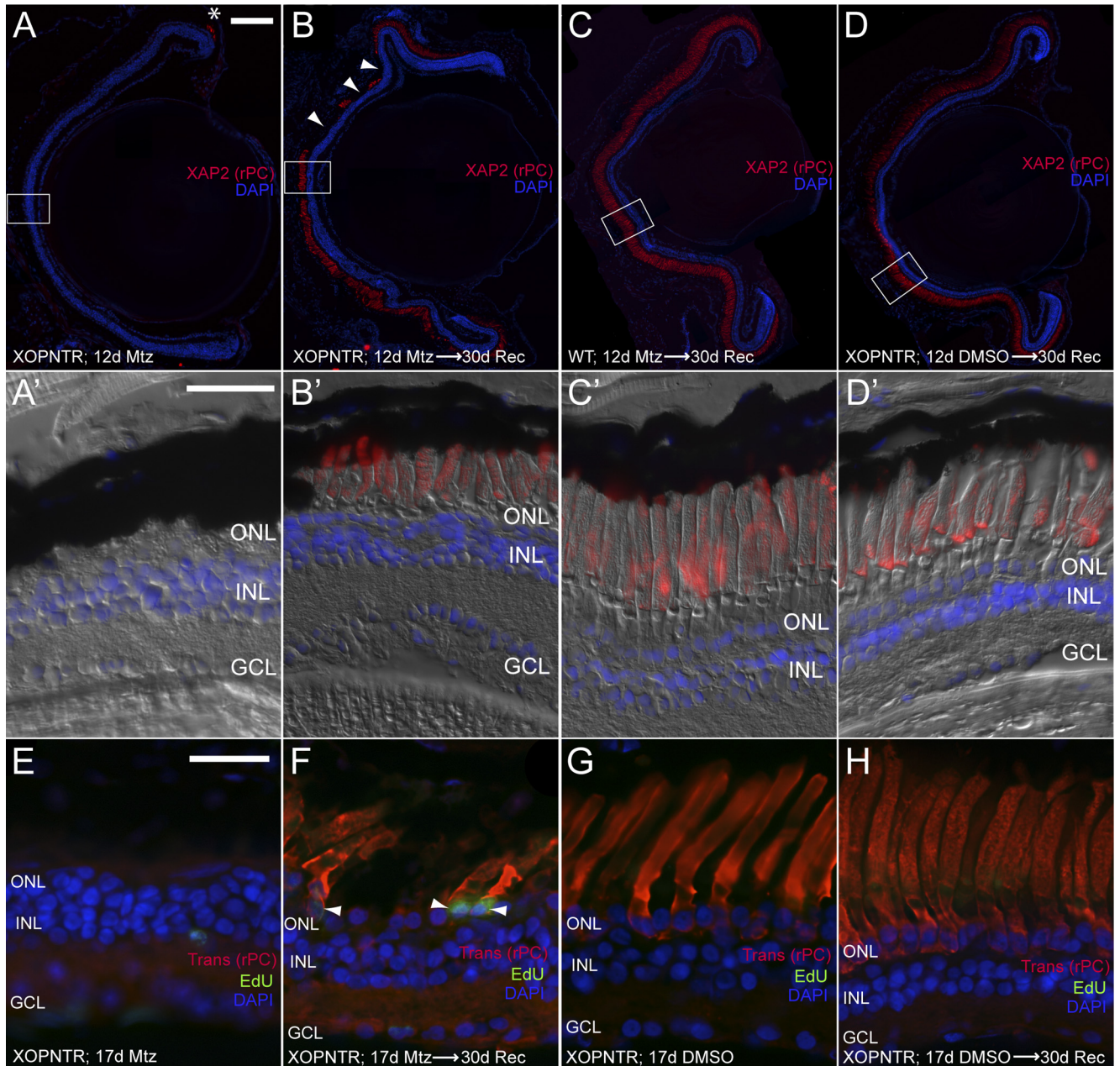


FIGURE 6. Rod photoreceptor regeneration in XOPNTR tadpoles. Stage 53 tadpoles were cultured in Mtz for 12 days and processed immediately (A, A') or were allowed to recover an additional 30 days (B–D') before immunohistochemistry. Retinal sections were stained for XAP2 to detect outer segments of rod photoreceptors. In XOPNTR animals treated with Mtz for 12 days, rod outer segments were only detected in the most peripheral retina (A, asterisk). After a 30-day recovery, rod outer segments were again detected in the central retina (B, B'), but they were shorter than rods of wild-type Mtz-treated (C, C') and XOPNTR untreated (D, D') tadpoles. (A'–D') Magnified views of the boxed regions in (A–D). (B, arrowheads) Regions lacking rod outer segments. Regenerated rods are EdU-positive. Mtz-treated (E, F) and untreated (G, H) stage 53 XOPNTR tadpoles were injected intra-abdominally with EdU, cultured for 17 days, and processed immediately (E, G) or allowed to recover in Mtz-free media for an additional 30 days (F, H) before immunohistochemistry. Retinal sections were stained to detect nuclei (DAPI; blue), rod photoreceptors (transducin; red), and cells that had passed through S-phase during treatment (EdU; green). Scale bars: 100 μm (A–D); 25 μm (A'–D', E–H).

activated, or both. For instance, XOPNTR tadpoles were continuously treated with metronidazole, whereas post-metamorphic frogs received periodic subcutaneous injections of the iCasp9 activator AP20187 (the effect of AP20187 on cone survival in tadpoles was not addressed). The discontinuous delivery method that must be used in older animals may not result in cone cell degeneration and death. Alternatively, the extent and rate of secondary degeneration may be age dependent. Frog cones may be more resistant to the effects of rod

ablation than are the cones of the tadpole retina. Examining the fate of cones in metronidazole-treated XOPNTR frogs and AP20187-treated iCasp9 tadpoles should distinguish between these possibilities.

Leakage of the cytotoxic-form of the drug into neighboring cells could also explain the loss of cones in XOPNTR animals. Several lines of evidence, however, suggest that this mechanism is unlikely to be driving cone loss in rod-ablated *Xenopus* retinas. First, cone cell loss was progressive, mimicking the

temporal sequence of morphologic changes observed in other animal RP models in which outer segments degenerate first, followed by the loss of cone soma.^{28,29} Second, cones continue to die in the absence of rods, which suggests cone loss is independent of the NTR-Mtz system because rods are no longer present to convert Mtz to its cytotoxic form. Consistent with this interpretation, cones lacking outer segments were observed in the ONL nearly 3 weeks after the last rods had been ablated (Fig. 4C''). Third, metronidazole was specifically developed as a substrate for NTR to avoid the prodrug-related death of neighboring cells observed with previous substrates. In cell culture studies, the death of neighboring cells was minimal, even under conditions in which targeted and nontargeted cells share gap junctions.⁴⁴ Fourth, a recent study investigating the regenerative response of the zebrafish retina to rod ablation found no evidence of cone cell death when using the NTR-Mtz system.¹³

In addition to cone loss, Müller glia hypertrophy was also observed in the retinas of Mtz-treated XOPNTR tadpoles. Expression of the Müller cell marker R5 (Fig. 5) and the intermediate filament protein vimentin (not shown) were dramatically increased in Mtz-treated animals. Enlarged Müller processes extend throughout the retina, most notably into the subretinal space (Fig. 5G). These changes mimic those observed in mammalian retinal degenerations.^{3,45} Zebrafish Müller glia also respond to rod loss by upregulating the expression of intermediate filaments such as glial fibrillary acidic protein.^{46,47} In contrast to *Xenopus*, however, extensive gliosis in the subretinal space has not been reported in fish. These results are intriguing given the distinct response of these two regenerative models to rod ablation. Cone loss is not observed in the rodless zebrafish retina.^{13,48} Rod ablation driven by misexpression of a membrane-targeted form of cyan fluorescent protein under the control of the *Xenopus* rhodopsin promoter did not result in cone degeneration.⁴⁸ Similarly, cone loss was not detected in Mtz-treated, rodless transgenic fish expressing NTR under the control of the zebrafish rod opsin promoter.¹³ In zebrafish, retinal damage results in the activation of Müller glia, which reenter the cell cycle to produce neuronal progenitors that differentiate into retinal neurons and heal the damaged region.^{46,49-54} In contrast to fish, retinectomy experiments in both premetamorphic and postmetamorphic *Xenopus* indicate transdifferentiating RPE is the source of new retinal neurons.^{10,11} The correlation between the extent of Müller cell hypertrophy and cone cell death may point to a role for gliosis in cone cell degeneration.

In *Xenopus*, rod ablation also resulted in a reduction in the thickness of the outer plexiform layer (Fig. 4C''); asterisks) observed in other models of photoreceptor degeneration.^{55,56} In contrast to nonregenerative models, however, we observed no statistically significant change in the number of INL or GCL cells in Mtz-treated tadpoles. Previous studies indicate that near complete cone cell loss is necessary for extensive neuronal remodeling, including the death of INL and GCL cells.²⁸ After 17 days of Mtz exposure, the number of cone cells was reduced to approximately 30% of wild-type levels, possibly explaining the lack of cell death in other retinal layers. In future experiments, it will be important to determine whether the late phases of degeneration (INL, GCL cell death, and neuronal remodeling) are observed in rodless and coneless XOPNTR tadpoles.

When given time to recover, the retinas of rod-ablated XOPNTR tadpoles generated new rod photoreceptors with outer segments; however, regeneration was not complete, possibly because of insufficient recovery time. Alternatively, secondary cellular or molecular changes in these regions might have permanently inhibited rod regeneration. Consistent with this hypothesis, rod regeneration appeared less robust in trans-

genic animals treated with Mtz for 17 days compared with 12-day treated animals (not shown). However, additional experiments will be necessary to distinguish between these two possibilities.

Two sources of new cells in the amphibian retina are the adult retinal stem cells of the CMZ and the retinal pigment epithelium (RPE). Additional experiments will be necessary to determine whether the CMZ, RPE, or an unidentified cell class is the source of the newly born rods. Recently, Müller glial cells have been speculated to contribute to the regeneration of the retina of higher order vertebrates, as occurs in teleost fish.^{52,57} However, our preliminary evidence shows no statistically significant difference in the number of mitotic or EdU-labeled Müller glial cells between Mtz-treated transgenic and control animals after 3, 5, or 10 days (data not shown). A more extensive study is necessary to conclusively determine whether Müller glial cells play a role in retinal regeneration.

During normal retinal development, cell classes are born in a stereotypical order. Retinal ganglion, horizontal, and cone cells are born early, followed by rods, bipolar, amacrine, and Müller cells. Are the mechanisms of rod regeneration distinct from those of retinal development? Are the early retinal cell fates skipped to directly generate rods in XOPNTR tadpoles? How rapidly is rod vision restored during regeneration? If retinal degeneration is allowed to progress, will regeneration no longer be possible? Or will rods, cones, INL, and RGCs all regenerate and reform the complex neural network necessary for functional vision? The rapid, synchronous degeneration of rods, their regeneration, and the ability to control the timing of these events, coupled with the behavioral assay, makes the XOPNTR model useful for studying the mechanisms regulating both retinal degeneration and regeneration.

Acknowledgments

The authors thank Barry Knox (SUNY Upstate Medical University), Steve Hobbs (Institute of Cancer Research, Sutton, Surrey, UK), and Bill Harris for providing the pXOP(-508/+41)GFP construct, F116 construct, and R5 antibody, respectively.

References

- Cottet S, Schorderet DF. Mechanisms of apoptosis in retinitis pigmentosa. *Curr Mol Med*. 2009;9:375-383.
- Milam AH, Li ZY, Fariss RN. Histopathology of the human retina in retinitis pigmentosa. *Prog Retin Eye Res*. 1998;17:175-205.
- Jones BW, Marc RE. Retinal remodeling during retinal degeneration. *Exp Eye Res*. 2005;81:123-137.
- Ripps H. Cell death in retinitis pigmentosa: gap junctions and the 'bystander' effect. *Exp Eye Res*. 2002;74:327-336.
- Lamba D, Karl M, Reh T. Neural regeneration and cell replacement: a view from the eye. *Cell Stem Cell*. 2008;2:538-549.
- Del Rio-Tsonis K, Tsonis PA. Eye regeneration at the molecular age. *Dev Dyn*. 2003;226:211-224.
- Fischer AJ. Neural regeneration in the chick retina. *Prog Retin Eye Res*. 2005;24:161-182.
- Reh TA, Tully T. Regulation of tyrosine hydroxylase-containing amacrine cell number in larval frog retina. *Dev Biol*. 1986;114:463-469.
- Hamm LM, Tam BM, Moritz OL. Controlled rod cell ablation in transgenic *Xenopus laevis*. *Invest Ophthalmol Vis Sci*. 2009;50:885-892.
- Vergara MN, Del Rio-Tsonis K. Retinal regeneration in the *Xenopus laevis* tadpole: a new model system. *Mol Vis*. 2009;15:1000-1013.
- Yoshii C, Ueda Y, Okamoto M, Araki M. Neural retinal regeneration in the anuran amphibian *Xenopus laevis* post-metamorphosis: transdifferentiation of retinal pigmented epithelium regenerates the neural retina. *Dev Biol*. 2007;303:45-56.

12. Zhao XF, Ellingsen S, Fjose A. Labelling and targeted ablation of specific bipolar cell types in the zebrafish retina. *BMC Neurosci.* 2009;10:107.
13. Montgomery JE, Parsons MJ, Hyde DR. A novel model of retinal ablation demonstrates that the extent of rod cell death regulates the origin of the regenerated zebrafish rod photoreceptors. *J Comp Neurol.* 2009;518:800–814.
14. Levine RL. La regenerescence de la retine chez *Xenopus laevis*. *Rev Can Biol.* 1981;40:19–27.
15. Anlezark GM, Melton RG, Sherwood RF, Coles B, Friedlos F, Knox RJ. The bioactivation of 5-(aziridin-1-yl)-2,4-dinitrobenzamide (CB1954)—I: purification and properties of a nitroreductase enzyme from *Escherichia coli*—a potential enzyme for antibody-directed enzyme prodrug therapy (ADEPT). *Biochem Pharmacol.* 1992;44:2289–2295.
16. Knox BE, Schlueter C, Sanger BM, Green CB, Besharse JC. Transgene expression in *Xenopus* rods. *FEBS Lett.* 1998;423:117–121.
17. Edwards DI. Nitroimidazole drugs—action and resistance mechanisms, II: mechanisms of resistance. *J Antimicrob Chemother.* 1993;31:201–210.
18. Roberts JJ, Friedlos F, Knox RJ. CB 1954 (2,4-dinitro-5-aziridinyl benzamide) becomes a DNA interstrand crosslinking agent in Walker tumour cells. *Biochem Biophys Res Commun.* 1986;140:1073–1078.
19. Viczian AS, Solessio EC, Lyou Y, Zuber ME. Generation of functional eyes from pluripotent cells. *PLoS Biol.* 2009;7:e1000174.
20. Moriya T, Kito K, Miyashita Y, Asami K. Preference for background color of the *Xenopus laevis* tadpole. *J Exp Zool.* 1996;276:335–344.
21. Kroll KL, Amaya E. Transgenic *Xenopus* embryos from sperm nuclear transplantations reveal FGF signaling requirements during gastrulation. *Development.* 1996;122:3173–3183.
22. Sive HL, Grainger RM, Harland RM. Early development of *Xenopus laevis*: a laboratory manual. Cold Spring Harbor, NY: Cold Spring Harbor Laboratory Press; 2000;ix:338.
23. Viczian AS, Vignali R, Zuber ME, Barsacchi G, Harris WA. XOTx5b and XOTx2 regulate photoreceptor and bipolar fates in the *Xenopus* retina. *Development.* 2003;130:1281–1294.
24. Mani SS, Batni S, Whitaker L, Chen S, Engbretson G, Knox BE. *Xenopus* rhodopsin promoter: identification of immediate upstream sequences necessary for high level, rod-specific transcription. *J Biol Chem.* 2001;276:36557–36565.
25. Moritz OL, Tam BM, Papermaster DS, Nakayama T. A functional rhodopsin-green fluorescent protein fusion protein localizes correctly in transgenic *Xenopus laevis* retinal rods and is expressed in a time-dependent pattern. *J Biol Chem.* 2001;276:28242–28251.
26. Chang WS, Harris WA. Sequential genesis and determination of cone and rod photoreceptors in *Xenopus*. *J Neurobiol.* 1998;35:227–244.
27. Harris WA, Messersmith SL. Two cellular inductions involved in photoreceptor determination in the *Xenopus* retina. *Neuron.* 1992;9:357–372.
28. Marc RE, Jones BW, Watt CB, Strettoi E. Neural remodeling in retinal degeneration. *Prog Retin Eye Res.* 2003;22:607–655.
29. Lin B, Masland RH, Strettoi E. Remodeling of cone photoreceptor cells after rod degeneration in rd mice. *Exp Eye Res.* 2009;88:589–599.
30. Gabriel R. Calretinin is present in serotonin- and gamma-aminobutyric acid-positive amacrine cell populations in the retina of *Xenopus laevis*. *Neurosci Lett.* 2000;285:9–12.
31. Ohnuma S, Philpott A, Wang K, Holt CE, Harris WA. p27Xic1, a Cdk inhibitor, promotes the determination of glial cells in *Xenopus* retina. *Cell.* 1999;99:499–510.
32. Seufert DW, Prescott NL, El-Hodiri HM. *Xenopus* aristaless-related homeobox (xARX) gene product functions as both a transcriptional activator and repressor in forebrain development. *Dev Dyn.* 2005;232:313–324.
33. Zaghoul NA, Moody SA. Changes in Rx1 and Pax6 activity at eye field stages differentially alter the production of amacrine neurotransmitter subtypes in *Xenopus*. *Mol Vis.* 2007;13:86–95.
34. Sakaguchi DS, Moeller JF, Coffman CR, Gallenson N, Harris WA. Growth cone interactions with a glial cell line from embryonic *Xenopus* retina. *Dev Biol.* 1989;134:158–174.
35. Carter-Dawson LD, LaVail MM, Sidman RL. Differential effect of the rd mutation on rods and cones in the mouse retina. *Invest Ophthalmol Vis Sci.* 1978;17:489–498.
36. Li T, Snyder WK, Olsson JE, Dryja TP. Transgenic mice carrying the dominant rhodopsin mutation P347S: evidence for defective vectorial transport of rhodopsin to the outer segments. *Proc Natl Acad Sci U S A.* 1996;93:14176–14181.
37. Gargini C, Terzibasi E, Mazzoni F, Strettoi E. Retinal organization in the retinal degeneration 10 (rd10) mutant mouse: a morphological and ERG study. *J Comp Neurol.* 2007;500:222–238.
38. Petters RM, Alexander CA, Wells KD, et al. Genetically engineered large animal model for studying cone photoreceptor survival and degeneration in retinitis pigmentosa. *Nat Biotechnol.* 1997;15:965–970.
39. Chang B, Hawes NL, Pardue MT, et al. Two mouse retinal degenerations caused by missense mutations in the beta-subunit of rod cGMP phosphodiesterase gene. *Vis Res.* 2007;47:624–633.
40. Kijas JW, Cideciyan AV, Aleman TS, et al. Naturally occurring rhodopsin mutation in the dog causes retinal dysfunction and degeneration mimicking human dominant retinitis pigmentosa. *Proc Natl Acad Sci U S A.* 2002;99:6328–6333.
41. Humphries MM, Kiang S, McNally N, et al. Comparative structural and functional analysis of photoreceptor neurons of Rho^{-/-} mice reveal increased survival on C57BL/6J in comparison to 129Sv genetic background. *Vis Neurosci.* 2001;18:437–443.
42. Machida S, Kondo M, Jamison JA, et al. P23H rhodopsin transgenic rat: correlation of retinal function with histopathology. *Invest Ophthalmol Vis Sci.* 2000;41:3200–3209.
43. Krebs MP, White DA, Kaushal S. Biphasic photoreceptor degeneration induced by light in a T17M rhodopsin mouse model of cone bystander damage. *Invest Ophthalmol Vis Sci.* 2009;50:2956–2965.
44. Bridgewater JA, Knox RJ, Pitts JD, Collins MK, Springer CJ. The bystander effect of the nitroreductase/CB1954 enzyme/prodrug system is due to a cell-permeable metabolite. *Hum Gene Ther.* 1997;8:709–717.
45. Jones BW, Watt CB, Frederick JM, et al. Retinal remodeling triggered by photoreceptor degenerations. *J Comp Neurol.* 2003;464:1–16.
46. Raymond PA, Barthel LK, Bernardos RL, Perkowski JJ. Molecular characterization of retinal stem cells and their niches in adult zebrafish. *BMC Dev Biol.* 2006;6:36.
47. Morris AC, Scholz TL, Brockerhoff SE, Fadool JM. Genetic dissection reveals two separate pathways for rod and cone regeneration in the teleost retina. *Dev Neurobiol.* 2008;68:605–619.
48. Morris AC, Schroeter EH, Bilotta J, Wong RO, Fadool JM. Cone survival despite rod degeneration in XOPS-mCFP transgenic zebrafish. *Invest Ophthalmol Vis Sci.* 2005;46:4762–4771.
49. Yurco P, Cameron DA. Responses of Muller glia to retinal injury in adult zebrafish. *Vision Res.* 2005;45:991–1002.
50. Fausett BV, Goldman D. A role for alpha1 tubulin-expressing Muller glia in regeneration of the injured zebrafish retina. *J Neurosci.* 2006;26:6303–6313.
51. Fimbel SM, Montgomery JE, Burket CT, Hyde DR. Regeneration of inner retinal neurons after intravitreal injection of ouabain in zebrafish. *J Neurosci.* 2007;27:1712–1724.
52. Bernardos RL, Barthel LK, Meyers JR, Raymond PA. Late-stage neuronal progenitors in the retina are radial Muller glia that function as retinal stem cells. *J Neurosci.* 2007;27:7028–7040.
53. Thummel R, Kassen SC, Montgomery JE, Enright JM, Hyde DR. Inhibition of Muller glial cell division blocks regeneration of the light-damaged zebrafish retina. *Dev Neurobiol.* 2008;68:392–408.
54. Thummel R, Kassen SC, Enright JM, Nelson CM, Montgomery JE, Hyde DR. Characterization of Muller glia and neuronal progenitors during adult zebrafish retinal regeneration. *Exp Eye Res.* 2008;87:433–444.
55. Aleman TS, Cideciyan AV, Sumaroka A, et al. Retinal laminar architecture in human retinitis pigmentosa caused by rhodopsin gene mutations. *Invest Ophthalmol Vis Sci.* 2008;49:1580–1590.
56. Yu DY, Cringle SJ, Su EN, Yu PK. Intraretinal oxygen levels before and after photoreceptor loss in the RCS rat. *Invest Ophthalmol Vis Sci.* 2000;41:3999–4006.
57. Karl MO, Hayes S, Nelson BR, Tan K, Buckingham B, Reh TA. Stimulation of neural regeneration in the mouse retina. *Proc Natl Acad Sci U S A.* 2008;105:19508–19513.